

Renormalized waves and discrete breathers in β -FPU chains

Boris Gershgorin¹, Yuri V. Lvov¹ and David Cai²,

¹ Department of Mathematical Sciences, Rensselaer Polytechnic Institute, Troy, NY 12180

² Courant Institute of Mathematical Sciences, New York University, New York, NY 10012

We demonstrate via numerical simulation that in the strongly nonlinear limit, the β -FPU system in thermal equilibrium behaves surprisingly like weakly nonlinear waves in properly renormalized normal variables. This arises because the collective effect of strongly nonlinear interactions effectively renormalizes linear dispersion frequency and leads to effectively weak nonlinear interaction among these renormalized waves. Furthermore, we show that the dynamical scenario for thermalized β -FPU chains is that spatially highly localized discrete breathers ride chaotically on spatially extended, renormalized waves.

The Fermi-Pasta-Ulam (FPU) system, a nonlinear lattice, was introduced in the classical work [1] to address fundamental issues of statistical physics such as equipartition of energy, ergodicity. The attempt to resolve the mystery of the FPU recurrence (the system did not thermalize as was expected but rather kept returning to the initial state [1]) has spurt many great mathematical and physical discoveries, such as the celebrated KAM theorem and soliton physics [2]. Recently, energy localization of lattice systems giving rise to discrete breather (DB) formation, was discovered [3]. The existence of DBs has been addressed rigorously [4, 5]. An important conceptual issue naturally arises: what is the role of DBs in the FPU dynamics [6–8]? Most of the results about DBs in β -FPU chains has so far addressed their roles in the transient state of weakly nonlinear regimes leading to thermal equilibrium [9–11].

In this Letter, we investigate the FPU dynamics in the strongly nonlinear limit and address the question of DB existence in thermal equilibrium. We demonstrate that, quite surprisingly, even for strong nonlinearity the β -FPU system in thermal equilibrium behaves like weakly nonlinear waves in properly chosen variables. Such behavior is due to the collective effect of strongly nonlinear interactions effectively renormalizing linear dispersion relation. This observation enables us to use a well-developed weak turbulence (WT) formalism [12] for the description of the β -FPU chains even in strongly nonlinear regime. In addition, we show via numerical simulation that in thermalized β -FPU chains the renormalized linear waves coexist with DBs — highly nonlinear, spatially localized excitations whose frequencies are well above the linear phonon band edge. These excitations were observed in the β -FPU chains during transient stages towards thermalization [9]. Here we show that DBs persist in the thermalized state as well.

The β -FPU chain is described by the Hamiltonian,

$$H = H_2 + H_4, \quad (1)$$

$$H_2 = \frac{1}{2} \sum_{i=1}^N p_i^2 + (q_i - q_{i+1})^2; \quad H_4 = \frac{\beta}{4} \sum_{i=1}^N (q_i - q_{i+1})^4,$$

where β is a *nonlinear parameter*, p_i and q_i , are the i -th particle momentum and displacement from the equilibrium position, respectively. The periodic boundary conditions are imposed. In terms of P_k and Q_k , the Fourier transforms of p_i and q_i , the Hamiltonian becomes

$$H = \frac{1}{2} \sum_{k=1}^{N-1} [|P_k|^2 + \omega_k^2 |Q_k|^2] + V(Q), \quad (2)$$

where $\omega_k = 2 \sin \frac{\pi k}{N}$ is the linear dispersion frequency and $V(Q)$ is the Fourier transform of H_4 . $V(Q)$ is a linear combination of various quartic products of Q_k 's and Q_k^* 's. We numerically integrate the equations of motion corresponding to Hamiltonian (1) to study possible dynamic scenario of the FPU. (We used 6-th order Yoshida algorithm [13] with the time step $dt=0.01$ and a 2-nd order symplectic and adaptive RK integrators. For each integrator we ensured a high degree of accuracy, e.g., the energy is conserved up to the 9-th digit for a runtime $T = 10^6$. We have verified that the choice of the integrator does not affect the results reported below.) Since the thermalized state is our primary interest we chose random initial data. Note that the behavior of the β -FPU in equilibrium is fully described by only one parameter βH [14] where H is the total energy of the system. We fixed $H = 200$ and varied β .

First, we measured power spectrum $\langle |a_k|^2 \rangle$ as a function of ω_k where $a_k = \frac{1}{\sqrt{2\omega_k}} (P_k - i\omega_k Q_k)$ and $\langle \cdot \rangle$ denotes the time averaging. We numerically studied the case of moderate and strong nonlinearities $\beta = 1, 8$ and 32 . Although it was expected that for weak nonlinearity $\langle |a_k|^2 \rangle = T/\omega_k$ where T is an effective temperature (Rayleigh-Jeans distribution for waves [12]), it is surprising to find that the same scaling holds even for strong nonlinearities as shown in Fig. 1. To obtain these plots the system was evolved for quite a long time $T_0 = 5 \times 10^5$ time units, which is much longer than the transient to thermal equilibrium [15]. The time window for averaging the power spectrum was chosen $\Delta T = 10^5$. To understand why $\langle |a_k|^2 \rangle \sim \omega_k^{-1}$, we computed the ω - k spectrum of $a_k(t)$ as shown in Fig. 2(a). In the weakly nonlinear limit it would have resonant peaks along a curve

given by the linear dispersion relation $\omega_k = 2 \sin(k\pi/N)$. When the nonlinearity is no longer small the resonances move to higher frequencies. Because of the nonlinear part $V(Q)$ the dispersion relation is renormalized as indicated by the sine-like structure of the resonance peaks (the solid line in Fig. 2(a)). We verified numerically that the main contribution of the nonlinear potential energy ($\sim 80\%$) comes from the terms $Q_k Q_l Q_m^* Q_s^*$ constrained on $k + l = m + s$. We note that when $k = m$ and $l = s$ or $k = s$ and $l = m$, these terms can be combined with the quadratic part of (2) to effectively renormalize the frequency ω_k . More specifically, Hamiltonian (2) can be rewritten as the sum of a new renormalized quadratic part and a remaining nonlinear part: $H = \tilde{H}_2 + \tilde{H}_4$ where $\tilde{H}_2 = \frac{1}{2} \sum_{k=1}^{N-1} (|P_k|^2 + \tilde{\omega}_k^2 |Q_k|^2)$ with the renormalized dispersion relation,

$$\tilde{\omega}_k = \eta \omega_k, \quad \eta = \sqrt{1 + \frac{3\beta}{2N} \sum_{l=1}^{N-1} \langle |Q_l(t)|^2 \rangle \omega_l^2}. \quad (3)$$

Note that the frequency renormalization factor η does not depend on k . Fig. 2(b) shows how the renormalized frequency $\tilde{\omega}_k$ depends on β . The upper curve was produced from the numerical spectrum - the abscissas of the peaks of the sine-like curves were measured (e.g., from Fig. 2(a) for $\beta = 1$, $\omega_{k=N/2} = 3.3$ for $N = 128$). The second curve was obtained using Eq. (3). Both dependencies seem to possess a scaling $\sim \beta^{0.2}$, which is represented by the dashed line for comparison. The discrepancy between the analytical and numerical curves can be attributed to the fact that in the derivation of formula (3) we took into account only 4-wave processes. In principal we can take into account higher order processes to obtain a more accurate analytical estimate of the renormalizing factor.

To further study the renormalization of interaction we measured the ratio of the quartic to quadratic parts of the energy *before* and *after* renormalization procedure (i.e., H_4/H_2 vs \tilde{H}_4/\tilde{H}_2) for different values of β with energy fixed (Fig. 2(c)). Fig. 2(c) shows that the effective renormalized linear part becomes more dominant. Therefore even for strongly nonlinear regimes, with β as large as 128, the renormalized waves have weakened interactions. Note that the resonance of $a_k(\omega)$ has a finite width (shown with the dashed lines in Fig. 2(a) which are the level of $\int |a_k|^2(\omega) d\omega / \max_w |a_k|^2$ for each k). We note that for $k = N/2$ (highest mode in the system) the resonances become the broadest. According to the theory of WT [12], the energy exchange among waves occurs on the resonance manifold given by $k_1 + k_2 = k_3 + k_4$ and $\omega_{k_1} + \omega_{k_2} = \omega_{k_3} + \omega_{k_4}$. Although one can show that there are no exact resonances in β -FPU chains on the discrete lattice, the near resonance interactions (i.e. $|\omega_{k_1} + \omega_{k_2} - \omega_{k_3} - \omega_{k_4}| < \delta$ where δ is a resonance width) can occur in the system. This allows us to use the WT theory if the interaction is considered to be weak. In order to characterize the system as weakly

nonlinear waves, the renormalized waves are described by the new normal variables $\tilde{a}_k = \frac{1}{\sqrt{2\tilde{\omega}_k}}(P_k - i\tilde{\omega}_k Q_k)$. The relationship between bare a_k and renormalized \tilde{a}_k is $a_k = \frac{1}{2} \left[(\sqrt{\eta} + \frac{1}{\sqrt{\eta}})\tilde{a}_k + (\sqrt{\eta} - \frac{1}{\sqrt{\eta}})\tilde{a}_{-k}^* \right]$. Under the random phases approximation for a_k [16] we have $\langle |\tilde{a}_k|^2 \rangle = \frac{2\eta}{1+\eta^2} \langle |a_k|^2 \rangle$. Therefore the power spectrum has scaling $1/\omega_k$ for both a_k and \tilde{a}_k . (Note in Fig. 1, $\langle |a_k|^2 \rangle$ is shown). As a consequence, the effective temperature, \tilde{T} , for the renormalized waves, is related to the bare temperature T by $\tilde{T} = [2\eta^2/(1+\eta^2)]T$.

The renormalization picture is further corroborated by the time evolution of each individual wave \tilde{a}_k . For the bare waves a_k , there are large temporal modulations in both modulus and phase as a result of strong nonlinear interaction among these modes on the linear dispersion time scale (as shown in Fig. 3(a) and (b)). In weakly nonlinear systems wave amplitudes and corresponding phases are expected to evolve slowly on the linear dispersion time scale. For renormalized waves (Fig. 3(c) and (d)) these modes indeed have characteristics of weakly interacting waves, with a small modulation in $|\tilde{a}_k|^2$ and phase. (Note that according to our definition $a_k = |a_k|e^{i(\phi+\omega_k t)}$ and the phase does not include the linear rotation.)

Now we turn to the numerical evidence for the persistence of DBs in the thermalized β -FPU chain. As observed before [9], there are DBs present in the transient state. As nonlinearity increases the duration of transient becomes shorter. After the energy redistributes among all the modes to achieve thermal equilibration, our simulations show that there still exist the spatially localized high frequency excitations. These DBs can interact with each other and may be destroyed by collision processes with other DBs or the renormalized waves. The spatial structure of these excitations very much resembles the idealized breather oscillations in the absence of spatially extended waves: they “live” above the high frequency edge of the dispersion band and their lifetime is sufficiently long (on the order of 10-100 DB oscillations) to behave like a quasiparticle. They can be clearly observed on the energy density plot which shows the time evolution of energy of each particle of the β -FPU chain: Fig. 4 is the energy density evolution for the transient (recording starting time $T_0 = 5 \times 10^2$) and thermalized ($T_0 = 5 \times 10^5$) states of the system respectively. Fig. 4(c) and (d) display the energy as a function of site at the initial recording time corresponding to Fig. 4(a) and (b) respectively. In the transient case (Fig. 4(a)) the spatially localized objects (dark stripes) that carry sufficiently large amount of energy are clearly observed. Fig. 4(c) is a snapshot of the energy density plot (4(a)) at the initial recording time. Here the DBs are seen as localized peaks [9]. After thermalization the spatial structure looks different (Fig. 4(b)). The system now consists of the renormalized

linear waves (straight cross-hatch traces in Fig. 4(b)). On the top of these waves, the localized structures similar to DBs manifest themselves as the wavy dark trajectories (in Fig. 4(b)). Although the snapshot (Fig. 4(d)) of the energy density plot (Fig. 4(b)) indicates that in thermal equilibrium the energy is more evenly distributed among particles, spatially localized structures are clearly observed.

Since there are renormalized waves in the system, which also carry energy, we need find a way to distinguish between these waves and DBs. We use a frequency filter that cuts out the lower side of the Fourier spectrum and leaves the high frequency part unmodified, i.e., $f(g(n, t)) = \Re F^{-1}(H_\omega(F(g)))$, where \Re denotes the real part, F is a time Fourier transform, H_ω annihilates all frequencies below ω_{cut} and $g(n, t)$ is a dynamical variable that is being filtered. By applying this filter to the displacement q_n to obtain $q_n^f \equiv f(q_n)$, we can show the existence of DBs even for strong nonlinearities, for example, $\beta = 25$ (and the same energy $H = 200$). Fig. 5(a) shows a clear example of a DB excitation reconstructed using the filtered variable q_n^f with $\omega_{cut} = 7$. Fig. 5(b) shows a typical spatial profile of the DB taken from Fig. 5(a), which strongly resembles the idealized DB [17]. The corresponding energy density distribution along with the distribution of filtered displacement $q_n^f(t)$ is displayed in Fig. 6(a) and (b), respectively. After the lower modes from the displacement q_n are filtered, one can clearly observe that the remaining high frequency oscillations are spatially highly localized, with the same characteristics as an idealized breather. These DBs coexist with renormalized linear waves in the system. Fig. 6(c) shows a q_n^f plot in zoomed region. The detailed time dynamics of a DB can be clearly seen here. As one of the main characteristics of breathers the values of q_n^f change signs periodically (as indicated by the alternating white and black spots along the trajectory) as the DB moves in space. We further point out that these DBs have spatial extent of 2 or 3 sites only, as seen in Fig. 6(c). Finally, for large systems we present the evidence that there is a turbulence of DBs as shown in Fig. 7, where it can clearly be seen that many DB excitations chaotically ride on renormalized linear waves.

In conclusions, in this Letter we have presented an interesting dynamical scenario of thermalized β -FPU chains:(i) For strong nonlinearity the linear dispersion relation is effectively renormalized, which allows one to treat even strongly nonlinear systems as if they were weakly nonlinear; (ii) In thermal equilibrium, on top of renormalized waves, the strongly nonlinear system is also characterized by the turbulence of discrete breathers.

Acknowledgments we thank Sergei Nazarenko for discussions; YL was supported by NSF CAREER grant 0134955, DC was supported by NSF DMS 0206779 and a Sloan fellowship.

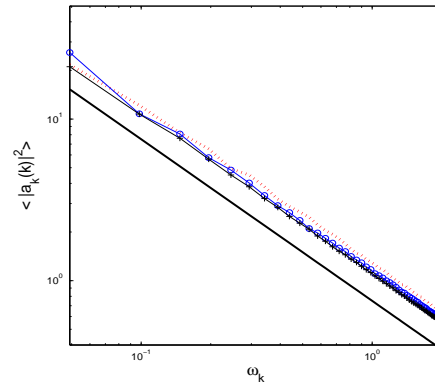


FIG. 1. Power spectra for the thermalized state for relatively strong nonlinearity $\beta = 1$ (dots), $\beta = 8$ (circles) and $\beta = 32$ (pluses). The thick solid line is $1/\omega_k$ for comparison.

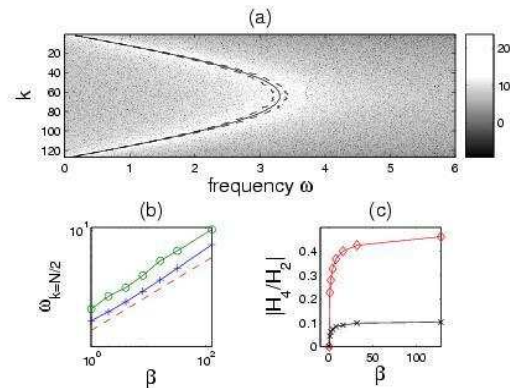


FIG. 2. (a) Density plot of spectrum ($\ln(|a_k(\omega)|^2)$ is plotted) . (b) renormalized linear frequency as a function of β : analytical predictions (pluses) and numerical measurements (circles). $\beta^{0.2}$ is shown for comparison (dashed). (c) effective nonlinearity as a function of β before (diamonds) and after (crosses) renormalization ($N=128$).

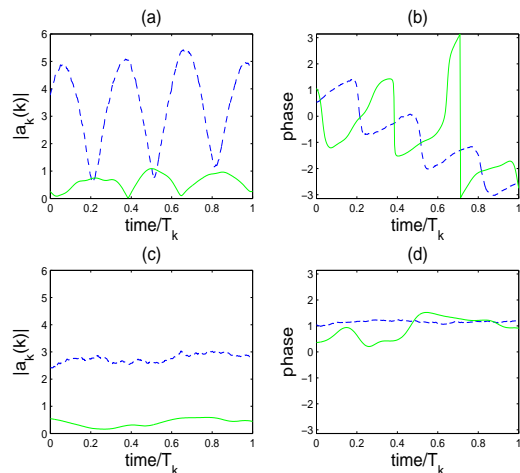


FIG. 3. (a) and (b) $|a_k|$ and phase respectively, using the bare linear dispersion $\omega_k = 2 \sin(\pi k/N)$. (c) and (d) $|\tilde{a}_k|$ and phase respectively using the renormalized dispersion $\tilde{\omega}_k$ (Eq.3). Dashed: $k = 1$, solid: $k = 20$. The dispersion time scale is described by $T_k = 2\pi/\omega_k$ for (a) and (b) and $T_k = 2\pi/\tilde{\omega}_k$ for (c) and (d).

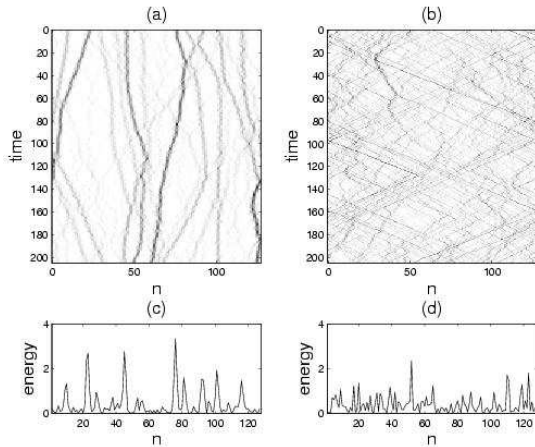


FIG. 4. Energy density evolution of the transient state (a) and (c), of the thermalized state (b) and (d), respectively ($\beta = 1$ and $H = 200$). In (a) and (b) the darker strips correspond to high energy localizations. (c) and (d) are the snapshots of energy density.

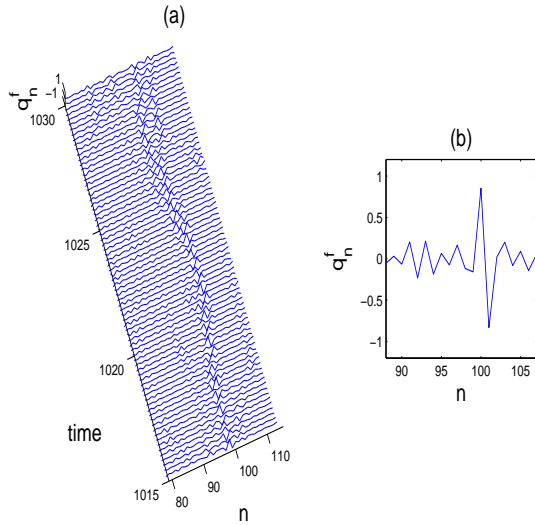


FIG. 5. (a) Evolution of a discrete breather in thermal equilibrium. (b) typical snapshot of the breather.

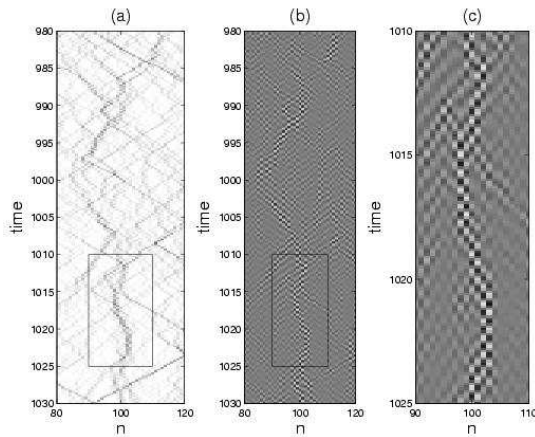


FIG. 6. Discrete breather in thermalization ($N=128$): (a) evolution of energy density, (b) $q_n^f(t)$, and (c) $q_n^f(t)$ in zoomed area indicated by the rectangle in (a), (b).

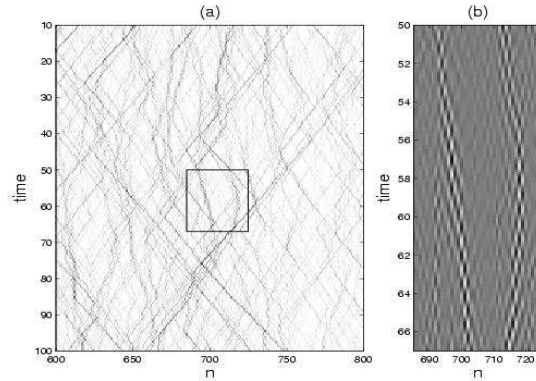


FIG. 7. Turbulence of discrete breathers ($N=1024$): (a) evolution of energy density, (b) zoomed in $q_n^f(t)$ of the area indicated by the rectangle in (a).

- [1] Fermi E., Pasta J. and Ulam S., Studies of nonlinear problems. Los Alamos Scientific Laboratory Report LA-1940 (reprinted in Fermi E. Collected papers Vol II, p 975, U.of Chicago Press, Chicago 1965).
- [2] For example, Ford J., *Phys. Rep.*, **213**, 271, (1992), Toda M., Theory of nonlinear lattice, Springer-Verlag, New York (1989).
- [3] S.Flach and C.R.Willis, *Phys. Rep.* **295**, 181 (1998) and references therein.
- [4] Aubry S., Kopidakis G. and Kadelburg V. *Dyn. Syst.* **B 1** 271298 (2001) .
- [5] James G. *C. R. Acad. Sci. Paris Ser. I Math.* **332** 581586 (2001).
- [6] Dauxois T., Ruffo S. and Torcini A., *Phys. Rev. E*, **56-6**, 6229, (1997).
- [7] Aoki K. and Kuznezov D. *Phys. Rev. Lett.*, **86**, 18, (2001).
- [8] Zhao H., et al. *Phys. Rev. Lett.*, **94**, 18, (2005).
- [9] Cretegny T., et al. *Physica D*, **121**, 109, (1998).
- [10] Schulman L.S., et al. *Phys. Rev. Lett.*, **88**, 22, (2002).
- [11] Kastner M. *Phys. Rev. Lett.*, **92**, 10, (2004).
- [12] Zakharov, V.E., Lvov V.S. and Falkovich G. Kolmogorov Spectra of Turbulence. Springer-Verlag, (1992).
- [13] Yoshida H., *Phys. Lett. A*, **150**, 262, (1990).
- [14] Poggio P. and Ruffo S., *Physica D*, **103**, 251, (1997).
- [15] To confirm that the system had reached the thermal equilibrium we monitored $C(t) = N(\sum E_i^2)/(\sum E_i)^2$ where E_i is the energy of the i -th particle [9]. The value of $C(t)$ is $O(N)$ when all the energy is concentrated around one site and is $O(1)$ when equipartition is reached. And $C(t)$ had values in the range $1 \sim 3$ in our simulations. Also various statistics of the system were verified to ensure that it reached the thermalized state with the Gibbs distribution [18]: (i) p_i of each particle distributed with pdf $P(p) \sim e^{-p^2/(2T)}$, and (ii) $y_i = q_i - q_{i-1}$ distributed with pdf $P(y) \sim e^{-(y^2/2+\beta y^4/4)/T}$.
- [16] Lvov Y., Nazarenko S. *Phys. Rev. E*, **69**, 066608, (2004).
- [17] Kivshar Y., et al. *Phys. Rev. B*, **58**, 5423 (1998).
- [18] Landau L., Lifshitz E. Statistical Physics (Course of theoretical physics Vol. 5), Pergamon, Oxford (1958).